ORIGINAL RESEARCH PAPER

The Institution of Engineering and Technology WILEY

Planning for resilience in power distribution networks: A multi-objective decision support

Pouya Jamborsalamati[1] | Rasoul Garmabdari[2] | Jahangir Hossain[3] | Junwei Lu[2] | Payman Dehghanian[4] (ORCID)

[1]School of Engineering, Macquarie University, Sydney, New South Wales, Australia

[2]School of Engineering, Griffith University, Nathan Campus, Nathan, Queensland, Australia

[3]School of Electrical and Data Engineering, University of Technology Sydney, Sydney, New South Wales, Australia

[4]Department of Electrical and Computer Engineering, The George Washington University, Washington, District of Columbia, USA

Correspondence

Pouya Jamborsalamati, School of Engineering, Macquarie University, Sydney, NSW 2109, Australia.
Email: pouya.jamborsalamati@hdr.mq.edu.au

Abstract

Power grid response against high-impact low-probability (HILP) events could be enhanced by (a) hardening mechanisms to boost its structural resilience and (b) corrective recovery and mitigation analytics to improve its operational resilience. Planning for structural resilience and attempts to find the optimal location of the Tie switches in radially operated power distribution networks that enable harnessing the network topology for maximised resilience against HILP disasters are focussed. This goal is achieved through a novel resilience-oriented multi-objective decision making platform, which employs a k-PEM based probabilistic power flow (PPF) algorithm. The proposed framework offers a decision making analytic embedded with the fuzzy satisfying method (FSM) that characterises the system resilience features, such as robustness, restoration agility, load criticality, and recovered capacity, to assess different network reconfiguration options and select the optimal solution for implementation. The aforementioned resilience features are formulated in nodal level and then aggregated over the entire system to characterise the system-level objective functions. The performance of the suggested framework is analysed on the IEEE 33-Bus test system under a designated HILP event, and the applicability on larger networks has been verified on the IEEE 69-bus test system. The results demonstrate the efficacy and applicability of the proposed framework in boosting the network resilience against future extremes.

1 | INTRODUCTION

Power grid resilience is defined as the ability of the system to avert possible event-driven damages, tolerate accidents, and engender a swift response and recovery following extreme disasters [1,2]. The reliable supply of electricity upon which modern society depends is at risk due to the unforeseen effects of a myriad of converging factors: elevated incidences and severity of outage-inducing high-impact low-probability (HILP) events, including, most notably, severe weather patterns and cyber attacks, sudden changes and proliferation of renewable resources, etc [3–5].

1.1 | Background and motivation

More frequent realisation of HILP events in power networks during the past decades has manifested significant importance

of maximising the grid preparedness against such incidents. Examples of HILP incidents in recent years are South Australian blackout in 2016 with 900 MW power outage due to extreme weather [6], major blackout in Brazilian grid in 2018 with 18,000 MW curtailed power in cascaded fault condition, outage in India in 2012 with 1423 TWh outage, severe power cut in the USA in 2015 with 180,000 customers affected due to abnormal weather condition, among many others [7,8].

Unlike the widely accepted standard metrics for reliability assessment in power distribution systems, for example, system average interruption duration index (SAIDI), system average interruption frequency index (SAIFI), and energy not supplied (ENS), a comprehensive evaluation framework which quantifies the *resilience* features such as preparedness, robustness, and restorative rapidity (among the others) is missing [6]. Resilience assessment could be focussed on a load point (node level) or the entire system (feeder-level) [9]. An effective

resilience metric could be utilised as an objective function in a wide variety of power grid long-term planning and short-term operation decisions to boost its capacity in dealing with the HILP incidents. Such a resilience metric needs to capture various aspects of the power grid behaviour ranging from the pre-event (infrastructural resilience) to the post-event (operational resilience) time frames, and its evaluation framework has to contain different quantitative and qualitative terms such as measures on energy capacity, rapidity, and economy [6].

1.2 | Related works

There are several research efforts that can be found in the literature on enhancing the resilience of power distribution grids to HILP events. In References [10–13], resilience-oriented outage management systems, which utilise microgrids and renewable energy resources to re-energise the critical loads following a natural disaster, are proposed where the focus has been primarily on enhancing the grid operational resilience. In References [9,14–16], novel evaluation frameworks with new metrics to quantify various resilience features are presented. Some of these efforts are founded based on the principle concept of graph theory for single-node level resilience evaluation in the network where parameters such as path redundancy, node connectivity, and resourcefullness are taken into account. Furthermore, parameters such as disruptive and restorative rapidity are suggested in References [6,17,18] focussing on the system-level (feeder-level) resilience evaluation.

While such efforts offer provisions for characterising the power distribution grid resilience and its swift operational response and recovery following an HILP incident, the flexible resources are assumed already planned and readily available to be utilised in practice. In References [19–22], preparedness against extreme events is pursued by optimal allocation of the grid-scale flexible resources (e.g. battery storage units, renewable resources, and electric vehicles) during extreme scenarios. Research outcome presented in Reference [23] shows analytical results of a risk assessment framework for weather-resilient power grid operation and control, where predictive measures for minimising the risk against forecasted weather-driven outages are suggested through effective utilisation of network topology control. Enhancing the grid operational resilience through changing the network topology requires additional switches that should be planned to be placed in strategic locations in the network, thereby facilitating rerouting the way electricity flows for swift response and recovery in dealing with the aftermath of HILP incidents. There has been multiple research studies conducted on optimising the location of Tie switches in distribution networks. It could be observed from References [24–27] that the Tie connection has been optimised based on various objective functions mostly from the reliability perspective to maximise DG loadability and load criticality. However, none of these Tie switch optimal placement strategies were designed to capture the resilience goals and requirements.

1.3 | Key contributions

Focussing on the pre-disaster preparedness and to pursue planning for structural resilience, this paper offers analytics that aim to maximise hardening against HILP events through resilience-oriented placement of Tie switches in radially operated power distribution networks. We approach this planning problem through a multi-objective optimisation framework that guides the optimal combination of the nodes to be re-connected following the network reconfiguration. In a modular architecture, a k-PEM based probabilistic power flow (PPF) algorithm is implemented to analyse the system operating state in each arrangement scenario of Tie switches across the network. The proposed analytics capture the load uncertainties in each restoration plan and utilises the fuzzy satisfying method (FSM) to make a final planning decision. The main contributions of this paper are illustrated in Table 1 and summarised below:

- Nodal-level resilience measures and metrics are proposed to quantify several resilience features that could be adopted by utilities for resilience-oriented planning and operation decision optimisation. The proposed resilience indices are employed in this paper in a multi-objective optimisation engine to optimally allocate the Tie switches in radial distribution networks.
- A modular framework for dynamic evaluation of the distribution network reconfiguration practices to maximise the resilience metrics is proposed. The developed framework utilises a k-PEM based PPF algorithm, which considers dynamic admittance matrix to evaluate the network operating condition at each reconfiguration plan.
- A diverse set of HILP scenarios is generated, followed by a detailed analysis of the results to demonstrate the efficacy of the proposed framework in boosting the network resilience against HILP disasters. The extensive discussions on the numerical results include both single-objective and multi-objective approaches, where the applicability of the proposed framework on both small-scale and large-scale networks is verified.

1.4 | Organisation of the paper

The rest of the paper is organised as follows: Section 2 presents the components which are utilised for resilience-oriented analysis in this paper. This includes: (a) introduction of the proposed resilience metrics and measures which are used to characterise the objective functions, (b) the objective function definitions for multi-objective optimisation, and (c) description of the k-PEM based PPF method used for calculation of the nodal resilience metrics in the network. Section 3 illustrates the workflow diagram and presents the details related to the proposed decision making platform. Section 4 concentrates on the case study results and the analysis of the findings. This Section also contains the optimal switch placement candidates and

TABLE 1 Comparison of resilience-oriented evaluation and optimisation platforms in the literature compared to this study

References	Level of resilience considered	Operational phase covered	Novel resilience metric developed?	NRC* considered?	NRA** considered?	NRS*** considered?	NRL**** considered?	Multi-objective optimisation conducted?
[9–12]	System	Post-event (Operational)	X	✓	✓	X	X	X
[8,13–15]	Nodal and system	Pre-event (Planning)	✓	✓	✓	✓	X	X
[5,16,17]	System	Post-event (Operational)	✓	✓	✓	✓	X	X
[18–22, 24–27]	System	Pre-event (Planning)	X	✓	✓	X	X	X
This paper	Nodal and system	Pre-event (Planning)	✓	✓	✓	✓	✓	✓

Notes: *Nodal restoration criticality, **Nodal restorability ***Nodal robustness ****Nodal restoration losses.

discussions on multi-objective approach to select the best candidate that satisfies all objective functions. Section 5 provides some discussions on the methodology and the computational efficiency of the proposed framework. Finally, Section 6 concludes the paper with point-by-point presentation of our contributions.

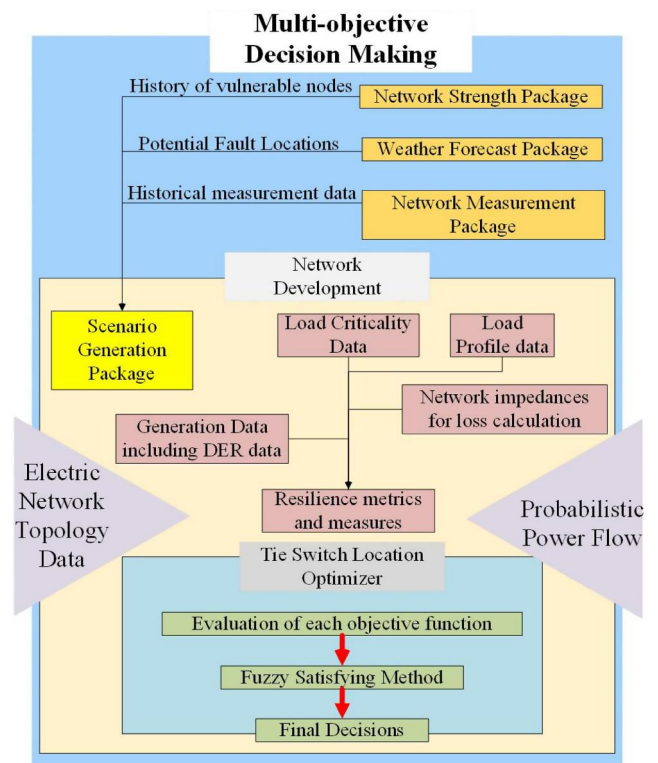## 2 | COMPONENTS FOR RESILIENCE-ORIENTED ANALYSIS

An overview of the proposed multi-objective decision making framework to optimally locate Tie switches in the network is demonstrated in Figure 1. The framework consists of components such as PPF, scenario generator, index calculator, and multi-objective optimiser, which are described in details in the following sections.

This paper proposes the analysis components as follows:

2.1 | Proposed resilience measures and metrics

An overview of the power system behaviour in the face of an HILP incident is conceptually demonstrated in Figure 2. $P(t)$ is the time-variant system behaviour function. At t_{NO}, an HILP event occurs, and the system goes to a performance degradation phase until t_{PD}. From t_{PD} to t_{OU} is represented as the system downtime with minimum number of customers served. At t_{OU}, the system response and recovery starts, and it takes multiple steps to realize a full restoration, where the system performance is migrated back to its normal operating condition. First partial recovery step leads to a temporary steady-state performance level indicated in Figure 2 from t_{ER_1} to t_{PR_1}, and the last step ends in the pre-event system performance level corresponding to the time instant t_{FR}.

As described earlier, there are three main categories of metrics that are commonly used for resilience assessments in

FIGURE 1 Overview of the main components proposed for resilience-oriented analysis of power distribution networks

power distribution systems: (i) time-based metrics, (ii) energy-based metrics, and (iii) economy-based metrics. Since our focus here is on the pre-event planning for structural resilience (i.e. grid hardening), time-based measures (reflecting the rapidity of the system restoration) are not taken into account. Restoration of a faulty radial feeder by connecting a Tie switch between the best pair of nodes is focused. Figure 3 demonstrates a generic view of a distribution system with a normally open Tie switch in the network. The proposed resilience metrics are defined over a single-node and summed

over the entire feeder to characterise the resilience objective functions. The suggested metrics are introduced as follows:

1. Nodal restoration criticality (NRC): NRC demonstrates the level of active power consumption and the type of the load (critical loads such as industry, hospitals, and fire stations) served at each load point. This metric represents the proportion of the critical loads covered by the restoration process to the total loads restored in the network. This index could be used to prioritise the nodes during the restoration process and is formulated for the node N in the network as indicated in Equation (1).

$$NRC^N = \left(P^{inj,N} = |\sum_{j\in\Omega_G^N} P_j^{Gen,N} - \sum_{i\in\Omega_L^N} P_i^{L,N}| \right) \times \frac{Pr_N}{P^{Tot}} \quad (1)$$

where $P^{inj,N}$ is the injected power at each node. $P_i^{L,N}$ and $P_j^{Gen,N}$ are the level of consumed and generated active power at node N, respectively. If there is any DER unit connected to a node, it will be reflected in the generated active power level of that particular node. Ω_L^N and Ω_G^N are the set of loads and generating units connected to node N, respectively; Pr_N is a utility-defined number assigned to node N depending on the type of the connected load, and P^{Tot} is the total amount of load restored by a restoration plan. Higher values of NRC reflect a

higher degree of criticality covered by a given restoration plan and is more desired.

2. Nodal robustness (NRS): NRS is defined by the difference between the nodal voltage profile before and after the restoration plan, the number of connected generating units ($|\Omega_G^N|$) and the number of incoming branches to node N ($|\Omega_B^N|$). The higher the difference in the nodal voltage profile before and after a restoration plan and the lower $|\Omega_G^N|$ and $|\Omega_B^N|$ are, the less robust is the distribution network to HILP incidents. Hence, NRS^N for node N is formulated as in (2).

$$NRS^N = \left(|V_{before}^{N^{th}} - V_{after}^{N^{th}}| \right) \times \frac{1}{|\Omega_B^N|} \times \frac{1}{|\Omega_G^N|} \quad (2)$$

3. Nodal restorability (NRA): NRA indicates the amount of load which would be restored by energising a single node in the healthy section of a faulty feeder. This restored load for the Nth node in a radial feeder is equal to the summation over all loads served at node N to the furthest downstream node in the feeder. Additionally, the number of outgoing branches from the node ($|\Omega_U^N|$) is a critical factor when evaluating the NRA. The NRA^N for the Tie switch connected to node N is formulated in Equation (3).

$$NRA^N = \left(\sum_{i\in\Omega_L^N} P_i^{L,N} + \sum_{j\in\Omega_L^{N+1}} P_j^{L,N+1} + \ldots \right.$$

$$\left. \ldots + \sum_{q\in\Omega_L^{EOF}} P_q^{L,EOF} \right) \times |\Omega_U^N| \quad (3)$$

where $P_q^{L,EOF}$ is the load served at the last node of the feeder.

4. Nodal restoration losses (NRL): NRL aims to characterise the power losses related to the restoration path created by closing the Tie switch during the restoration process. NRL^N
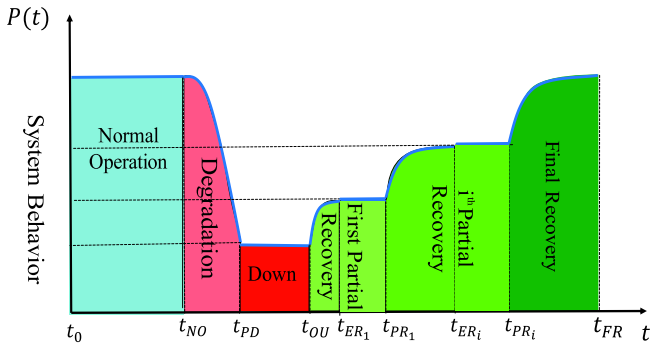

FIGURE 2 Overview of the system behaviour subject to an high-impact low-probability (HILP) event
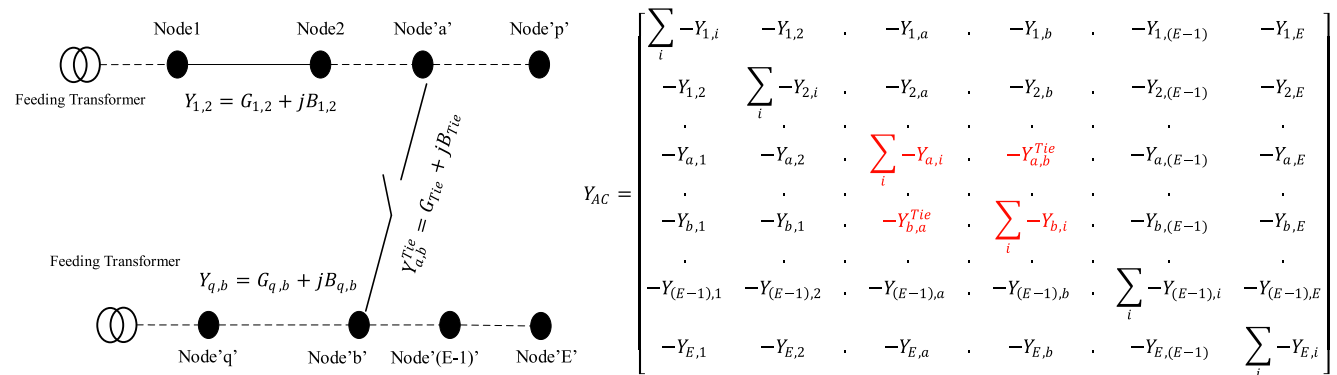

FIGURE 3 Generic view of a radial distribution network with Tie switches considered for formation of the Y_{AC} matrix

indicates the restoration losses in a radial feeder, where the Tie switch is connected to node N, as shown in Equation (4)

$$NRL^N = P_N^{Loss} + P_{N+1}^{Loss} + \cdots + P_{EOF}^{Loss} + P_{Tie}^{Loss} \quad (4)$$

where P_N^{Loss} is the power losses at Segment N (between nodes N and $N+1$), P_{EOF}^{Loss} is the power losses in the last segment of the feeder, and P_{Tie}^{Loss} is the power losses corresponding to the path created by closing the Tie switch.

2.2 | Objective functions

The above metrics of resilience are here used to form the objective functions. The optimisation engine embodies a mixed integer linear programing (MILP) formulation that aims to find the optimal location of the Tie switch in the network, primarily planned to enhance the network resilience against HILP disasters.

1. System-wide robustness: The first objective function utilises the NRS^N metric to minimise the system-level performance degradation when subjected to an HILP event. NRS^N is defined over a single node in Equation (2) and needs to be summed over the entire nodes in the network for a system-wide analysis. The objective function is formulated below subject to a set of system and operational constraints:

$$\min\left(NRS^{Tot} = \sum_{N \in E} \alpha_N NRS^N\right) \quad \alpha_N \in \{0,1\} \quad (5)$$

$$NRS_{min}^N < \alpha_N . NRS^N \leq NRS_{max}^N \quad \forall N \in \{E\} \quad (6)$$

$$P_{min}^{Gen,N} \leq \alpha_N . P^{Gen,N} \leq P_{max}^{Gen,N} \quad \forall N \in \{E\} \quad (7)$$

$$P_{min}^{Flow,k} \leq \alpha_N . P^{Flow,k} \leq P_{max}^{Flow,k} \quad \forall k \in \{\Omega_T\} \quad (8)$$

$$\sum_{q \in \Omega_U^N} P_q^{Flow,k} + \sum_{i \in \Omega_L^N} P_i^{L,N} = \sum_{j \in \Omega_G^N} P_j^{Gen,N} \quad (9)$$

$$\alpha_N \in \{0,1\} \quad \forall N \in \{E\} \quad \forall k \in \{\Omega_T\} \quad (10)$$

where $P^{Flow,k}$ is the power flow in branch k, Ω_T is the set of network branches, and α_N is a binary variable which indicates whether a node is involved in the restoration process. Constraint (6) ensures that the voltage difference in all nodes remains within a certain limit following the restoration process. The output power of generating units is limited to their physical capacities in Equation (7). Constraint (8) enforces that the electricity flow in distribution lines, involved in the service restoration, is bounded by their capacities. The power balance constraint at each node is set in Equation (9).

2. System-wide restoreability: This objective function aims to maximise the amount of the restored load via

connection of a Tie switch in a restoration plan and is built on the suggested NRA^N metric. As indicated in Equation (3), the NRA^N represents the summation of all loads restored in the feeder by energising the single-node N. The objective function is formulated in Equation (11) subject to several system and operational constraints:

$$\max\left(NRA^{Tot} = \sum_{N \in E} \sum_{i \in \Omega_L^N} \beta_N P_i^{L,N}\right) \quad \beta_N \in \{0,1\} \quad (11)$$

$$NRA_{min}^N \leq \alpha_N . NRA^N \leq NRA_{max}^N \quad \forall N \in \{E\} \quad (12)$$

$$P_{min}^{Gen,N} \leq \alpha_N . P^{Gen,N} \leq P_{max}^{Gen,N} \quad \forall N \in \{E\} \quad (13)$$

$$P_{min}^{Flow,k} \leq \alpha_N . P^{Flow,k} \leq P_{max}^{Flow,k} \quad \forall k \in \{\Omega_T\} \quad (14)$$

$$\beta_N \in \{0,1\} \quad \forall N \in \{E\} \quad \forall k \in \{\Omega_T\} \quad (15)$$

Constraint (12) ensures that the restored loads do not exceed a threshold—that is to avoid a possible overload in a neighbouring feeder—and is set to be higher than a minimum expected value. NRA_{max}^N is determined by the capacity of a feeding transformer in the neighbour feeder which will export power to the faulty feeder when a Tie switch is connected. Constraints (13)–(15) are employed to avoid exceeding capacities of the distribution lines and generation units. β_N is a binary variable indicating whether a node is involved in the restoration process.

3. Restoration of critical load points: A higher load outage recovery through a restoration plan does not necessarily result in recovery of highly critical load points. This objective function maximises the load criticality picked by a restoration plan and is formulated in Equation (16):

$$\max\left(NRC^{Tot} = \sum_{N \in E} \gamma_N NRC^N\right) \quad \gamma_N \in \{0,1\} \quad (16)$$

$$NRC_{min}^N \leq \gamma_N . NRC^N \leq NRC_{max}^N \quad \forall N \in \{E\} \quad (17)$$

γ_N is a binary variable to select the nodes involved in the restoration plans. Constraint (17) summarises various operational constraints and ensures a minimum recovery of critical loads via a restoration plan. Furthermore, the criticality picked by a restoration plan must not exceed a threshold, which otherwise violates the physical capacity of lines and generating units.

4. Restoration losses: This objective function is characterised to minimise the active power losses in the network resulted by adoption of a restoration plan and connection of a Tie switch. The NRL^N, presented in Section 2, represents the network total power losses in the restoration path.

$$\min\left(NRL^{Tot} = \sum_{i\in\Omega_T} \zeta_i P_i^{Loss}\right) \qquad \zeta_N \in \{0,1\} \qquad (18)$$

$$NRL_{min}^N \le \zeta_N.NRL^N \le NRL_{max}^N \qquad \forall\, N \in \{E\} \qquad (19)$$

ζ_i is a binary variable to select distribution lines which are used during the service restoration process. Operational constraints (12)–(14) are aggregated in Equation (19), which limit the amount of network losses in a restoration path. The thermal capacitance of the distribution lines and the physical capacity of generating units must not be violated via a restoration plan.

2.3 | Probabilistic power flow

PPF is an essential component of the power system planning with uncertainties taken into account [28]. First, the power flow along with the essential constraints (e.g. radiality constraint) considered in this work are presented. The description of the uncertainty modelling and PPF come next in this subsection.

2.3.1 | Power flow and essential constraints

Power flow has been formulated and discussed in many references, but the substantial equations are as follows:

$$P_i^{net} = \sum_{g\in G} P_i^g - \sum_{d\in D} P_i^d \qquad (20)$$

$$Q_i^{net} = \sum_{g\in G} Q_i^g - \sum_{d\in D} Q_i^d \qquad (21)$$

$$P_i^{net} = V_i \sum_{j\in N_b} Y_{ij} V_j Cos(\delta_i - \delta_j - \theta_{ij}) \qquad (22)$$

$$Q_i^{net} = V_i \sum_{j\in N_b} Y_{ij} V_j Sin(\delta_i - \delta_j - \theta_{ij}) \qquad (23)$$

where d and g are indices for loads and generating units at each bus running from 1 to D_i and 1 to G_i, respectively. P_i^{net} and Q_i^{net} are the net active power and reactive power injection at bus i, respectively. Inequality constraints represent maximum and minimum allowable limits for bus voltages at PQ buses and reactive power production of generating units at PV buses as follows:

$$V_i^{min-PQ} \le V_i^{PQ} \le V_i^{max-PQ} \qquad (24)$$

$$V_i^{min-PV} \le V_i^{PV} \le V_i^{max-PV} \qquad (25)$$

Radial topology of the network must be maintained over all time, and this constraint is formulated as follows:

$$\sum_{(i,j)\in\Omega_T} Conn_{i,j}^t = |E| - \lambda^t \qquad \forall\, t \in \{T\} \qquad (26)$$

$$\sum_{(ji)\in\omega_T} fl_{ji}^t - \sum_{(ij)\in\omega_T} fl_{ij}^t = Import_i^t \qquad \forall\, t \in \{T\} \qquad (27)$$

$$\sum_{(ij)\in\omega_T} fl_{ij}^t - \sum_{(ji)\in\omega_T} fl_{ji}^t = fg_i^t \qquad \forall\, t \in \{T\} \qquad (28)$$

$$Conn_{i,j}^t.Tie \le fl_{ij} \le Conn_{i,j}^t.Tie \qquad \forall\, t \in \{T\} \qquad (29)$$

where $Conn_{i,j}^t$ denotes the connection status of branch (i,j) at time t (1 if the branch is connected, 0 otherwise). Ω_T represents the total number of branches in the network. $|E|$ is the number of all nodes. λ^t is the number of islands formed due to the network reconfiguration at time t. fl_{ij} is the fictitious flow on branch (i,j) at time t. fg_i^t is the fictitious supply at source node i at time t. $Import_i^t$ is the fictitious imported power by the candidate tie connection. Tie is the set of possible tie connections to Node i and T is the set of time periods. Two conditions need to be satisfied to maintain the network radiality at all times: (i) the number of online branches in each restoration plan should be equal to the total number of nodes in the restoration plan and (ii) all load nodes should be connected to a determined source node in each restoration plan. The first requirement is met in constraint (26) through the concept of fictitious source and load nodes. The latter is fulfiled in constraints (27)–(29).

2.3.2 | Uncertainty modelling

Uncertainty is one of the major factors which escalate the risk on any decision made in power systems [29]. Due to numerous uncertainties in power systems, such as in the system demand growth, power system studies need to be equipped with tools for uncertainty modelling. There are several approaches taken in the literature to address the uncertainty modelling in power systems. Monte–Carlo Simulation (MCS) is one of the main methods to model the uncertainties precisely. However, a large number of simulations and higher computational burden is the drawback of this approach [29]. Methods such as multi-linear model, the cumulant and Von Mises functions, and the Gram–Charlier expansion method require mathematical assumptions to accomplish [30–32]. First-order second-moment method (FSOMM) is an approximate approach which relies heavily on derivative of random variables [32]. Among all, the point estimate method (PEM) has gained attraction in recent research studies with the following main advantages [33]:

- Although PEM employs a deterministic routine for uncertainty modelling, its computational burden compared to the other similar probabilistic problem solving methods such as MCS is significantly lower.
- Lack of data cannot crucially affect the effectiveness of the PEM method as the random input variables are approximated with their first three moments.

2.3.3 | PEM algorithm

The PEM is adopted to compute the moments of random variables Y which are a function of n random input variables X, that is, $y = F(x_1, x_2, ..., x_n)$ These statistical moments are the mean (i.e. the first moment around the source) and the variance (i.e. the second moment with reference to the mean). In our resilience-oriented problem for placement of Tie switches, the input and output random variables can be indicated as follows:

$$X = [P_i^{L,N}, |V_{before}^N - V_{after}^N|] \tag{30}$$

$$Y = [NRC, NRS, NRA, NRL] \tag{31}$$

Each input random variable is concentrated on K points, which are made available by the first three moments of the input random variables. K identifies different variants of PEM in the K-PEM method [29]. Due to the required accuracy and computational burden, 2-PEM is adopted in this work for uncertainty modelling. The statistical data of the output random variables can be calculated with regards to these points and the relation function between the input and the output variables. The following steps are taken to implement the 2-PEM-based PPF procedure [29]:

- A suitable probability distribution function (PDF) is assigned to each probabilistic variable.
- $E(Y) = E(Y^2) = 0$
- The crucial parameters of the 2-PEM have to be calculated based on the following equations:

$$\xi_{k,1} = +\sqrt{n} \quad \xi_{k,2} = -\sqrt{n} \tag{32}$$

$$P_{k,1} = P_{k,2} = \frac{1}{2n} \tag{33}$$

where $\xi_{k,1}$, $\xi_{k,2}$, $P_{k,1}$, and $P_{k,2}$ represent the locations and probabilities of concentrations, respectively.

- k is set to one ($k = 1$).
- $x_{k,1}$ and $x_{k,2}$ have to be determined and the deterministic power flow has to be deployed with regards to the input vector X.

$$x_{k,1} = \mu_{X,k} + \xi_{k,1}.\sigma_{X,k} \quad x_{k,2} = \mu_{X,k} + \xi_{k,2}.\sigma_{X,k} \tag{34}$$

$$X = [\mu_{k,1}, \mu_{k,2}, ..., x_{k,i}, ..., \mu_{k,n}] \qquad i = 1, 2 \tag{35}$$

where $\mu_{x,k}$ is the mean value of the kth input random variable.

- In this step, $E(Y)$ and $E(Y^2)$ need to be updated.

$$E(Y)^{(k+1)} \cong E(Y)^{(k)} + \sum_{i=1}^{2} P_{k,i}.h(X) \tag{36}$$

- $k = k + 1$ should be conducted, and steps after $k = 1$ should be repeated until all random variables are covered.
- Standard deviation and the expected value of Y must be calculated from the following equations:

$$\mu_y = E(Y) \tag{37}$$

$$\sigma_y = \sqrt{E(Y^2) - \mu_y^2} \tag{38}$$

3 | MULTI-OBJECTIVE DECISION PLATFORM FOR RESILIENCE-ORIENTED PLACEMENT OF TIE SWITCHES

This section describes the modular resilience-oriented framework developed to solve the optimisation problem presented in Section 2. The developed framework utilises the k-PEM based PPF and tries to iteratively maximise the proposed R index of resilience. The key element in the proposed optimisation platform is the dynamic admittance matrix (Y_{AC}), which determines the distribution network topology in each placement scenario of the Tie switch. The overall formation of Y_{AC} for a generic radial network with E number of nodes and a Tie switch connected between nodes a and b is illustrated in Figure 3. The Y_{AC} shown in this figure is generic and the same approach could be applied to construct the Y_{AC} in radial networks with several Tie switches connecting multiple pairs of nodes. One needs to note that $Y_{i,j} = Y_{j,i} = G_{i,j} + jB_{i,j}$; where $G_{i,j}$ and $B_{i,j}$ are the conductance and the susceptance of the lines between nodes i and j, respectively. $Y_{a,b}^{Tie}$ is the admittance of the tie-line that is set online when closing the normally open Tie switch connecting nodes a and b in the network and is equal to $Y_{a,b}^{Tie} = Y_{b,a}^{Tie} = G_{Tie} + jB_{Tie}$; where G_{Tie} and B_{Tie} are the conductance and the susceptance of the Tie-line, respectively. In a generic format, a Tie switch is connected between nodes a and b, which affects the elements on the corresponding rows and columns of the (Y_{AC}) matrix by $Y_{a,b}^{Tie}$ (admittance of the Tie-line). The affected elements in the admittance matrix are highlighted in red in Figure 3. The size and the elements of the admittance matrix can change depending on the grid topology following a reconfiguration plan.

Figure 4 demonstrates the proposed multi-objective decision making framework for resilience-oriented placement of the Tie switches in radial power distribution networks. The proposed framework consists of four main stages as follows: (i) Scenario Generation, (ii) k-PEM-Based PPF, (iii) index calculator, and (iv) multi-objective optimisation and decision making.

Stage 1: receives the network measurements along with its topology and contains generation and distribution system datasets, through which the admittance matrix for the imported Y_{AC} is formed. A set of candidate nodes are selected to

go black (offline) as a result of an HILP incident scenario. All possible pairs of nodes, characterised by a node in restorable section of the network and a node in the non-affected physically accessible section of the network, are stored as a set of Tie switch site candidates. For each Tie switch placement candidate, the Tie elements in Y_{AC} are added as shown in Figure 3 (red elements). The Y_{AC} is generated for all possible Tie switch locations, which is used as the input to the next stage.

Stage 2: The PPF, described in Section 2.3, runs at this stage for each generated Y_{AC} from Stage 1 and returns the mean values of the output variables.

Stage 3: Resilience metrics introduced earlier in Equations (6)–(9) are evaluated system wide. Stage 3 imports the results of PPF for each Tie switch location candidate and calculates the *NRC*, *NRS*, *NRA*, and *NRL* across the network. Such results are then used in a multi-objective decision platform to find the optimal solution.

Stage 4: Among various multi-objective decision making techniques, non-dominated sorting genetic algorithm II (NSGA-II), with demonstrated efficacy and usability [34], is employed. Utilising NSGA-II results in a set of non-dominant solutions (Pareto optimal sets) for all objective functions. The process starts with producing the first parent population followed by ranking them based on the concept of non-dominance. Classic operators (crossover and mutation) generate the children population to be used in combination with parent population for the next generation of Pareto solutions until a termination criterion is satisfied [34]. FSM is next employed to chose between all optimal Pareto solutions

(optimal Tie switch locations) [35,36] considering a trade-off between all objectives introduced in Section 2.3. The FSM approach is a mathematical expression tool that represents human judgements [36]. This approach is pursued as different user preferences and the decision maker (e.g. the utility) judgements may otherwise render the decision framework imprecise. The main advantages of employing the FSM include [37]: (a) user-defined targets for each objective (called satisfaction levels), which are the inputs to the multi-objective decision making optimisation module, (b) the fuzzy-based decision making measures the certainty or uncertainty of membership of an element of the set, which offers higher flexibility to the electric utilities for selecting the desired elements, (c) the reasoning process has low computational burden in case of applying the proposed framework in real-time or to large-scale systems, (d) fuzzy-based decision making usually has a shorter development time than the conventional methods and easier to implement in real world practices. The step-by-step procedure of the FSM implementation is introduced as follows:

1. Membership function (MSF): MSF includes a set of attributes to each objective function, indicating the significance level assigned to a given objective by a decision maker. MSF values are selected between zero and one, zero representing the lowest priority and one the highest. For instance, in a minimisation problem, the MSF equals to zero at the summit point of the objective function and is equal to one at its minimum. The linear MSF utilised in here is expressed in Equation (25).
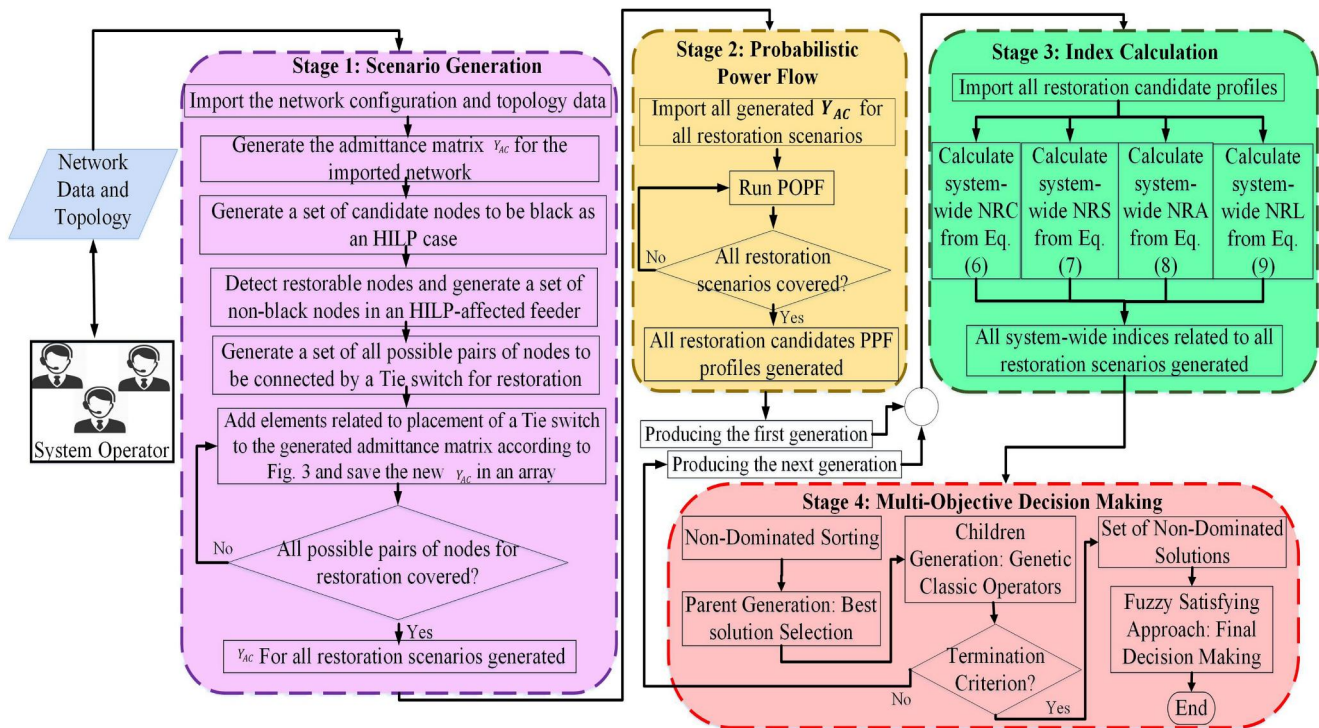

FIGURE 4 The overall architecture of the proposed multi-objective decision platform for Tie switch placement in power distribution networks

$$\mu_{f_i}(X) = \begin{cases} 0 & \text{if } f_i(X) > f_i^{max} \\ \dfrac{f_i^{max} - f_i(X)}{f_i^{max} - f_i^{min}} & \text{if } f_i^{min} \leq f_i(X) \leq f_i^{max} \quad (39) \\ 1 & \text{if } f_i(X) < f_i^{min} \end{cases}$$

2. Decision maker: The final decision is made considering the user-defined satisfaction levels for each MSF as indicated in Equation (26). This optimisation minimises the τ-norm deviations from the designated satisfaction levels considering the MSF of all solutions.

$$\min_{X \in SolutionSet} \left(\sum_{i \in R} |\mu_{d_i} - \mu_{f_i}(X)|^{\tau} \right) \qquad \tau \in \{1, \infty\} \qquad (40)$$

4 | CASE STUDY AND EVALUATION RESULTS

In order to showcase the efficacy of the proposed multi-objective decision making framework, the IEEE 33-bus test system with network data (distribution line impedances, load profiles, and generation details) taken from Reference [38] is selected as the first test case. All the proposed metrics are evaluated in per-unit values (i.e. unit-less). A major HILP event is simulated as graphically illustrated in Figure 5. We aim to study such extreme scenarios to demonstrate how the system resilience can be improved by grid hardening planning solutions for optimal allocation of Tie switches across the network and with various customisable risk appetites. The results in this section are presented in two main categories: first, single-objective calculations of the objectives are demonstrated; this is followed by the proposed multi-objective approach to finalise the decision making outcome.

4.1 | Single-objective solutions for tie switch placement and discussions

This sub-section describes the details of the studied HILP event and the possible Tie switch placement candidates based on each individual objective function defined in Section 2.3 for effective restoration. Figure 5 displays different zones in the network where facing a simulated HILP event. Nodes 7–10 highlighted in red (Zone 2) are affected by the HILP event and nodes 11–18 coloured in blue (Zone 3) are the restorable sections of the network. Zone 3 could be re-energised through a created path by closing a Tie switch to be installed in one of the candidate locations (green-dotted lines). While the presented decision making framework is generic enough to be applied to any HILP scenario with different spatiotemporal characteristics and severity levels, it finds 96 candidate locations for a Tie switch placement for
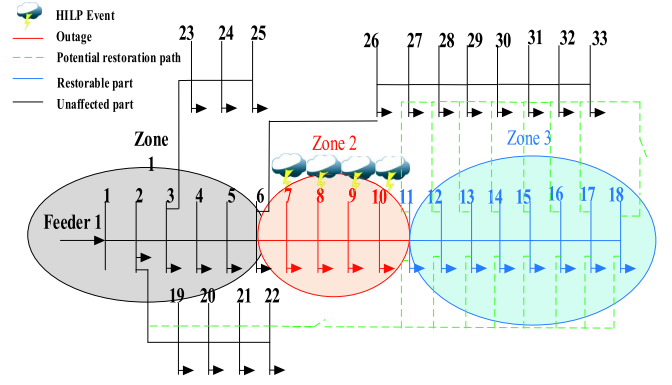

FIGURE 5 Single-feeder network affected by an HILP event

the designed HILP scenario in this paper. The connection nodes of these Tie switch location candidates are demonstrated in the first column of Table 2 as 'Potential Tie Switch Locations'. The grey zone in Figure 5 represents the unaffected section of the feeder, which would be used as the main restoration resource.

The k-PEM-based PPF runs for each Tie switch location to achieve the corresponding system profile following the plan implementation. Figure 6 displays the voltage profile in the test system subject to black nodes (Node 7–10) for all possible restoration plans (i.e. the 96 Tie switch placements). It could be observed from Figure 6 that Nodes 7–10 remain black due to the HILP outage scenario while Nodes 11–18 are restored within various Tie switch connection plans. Note that based on the sequential relay coordination and operation of the protection devices in the distribution feeder, the designed restoration process is selective, meaning that either the entire healthy part of the faulty feeder or a portion of it are considered for restoration through the suggested reconfiguration plans. In other words, the protection devices have isolated the faulty segments of the feeder following the HILP incident and each non-faulty segment could be restored by (1) closing the corresponding line breakers and (2) closing the potential Tie switch in each restoration plan.

Each resilience metric is evaluated at the nodal level for each Tie switch placement scenario and summed over the entire feeder for system-wide performance analysis. Table 2 presents the results corresponding to each individual objective function defined in Section 2.3. The last column of this table illustrates the results of single-objective Tie switch placement, indicating the objective function which is optimised by the Tie switch connection between the nodes listed in the first column of this table. Since the critical loads covered in multiple restoration plans (Tie switch locations) could be the same, there are multiple solutions for considering NRC solely. Set of single-objective solutions includes all the Tie switch locations where one of the following conditions is satisfied: NRC is maximised (multiple solutions), or NRS is minimised (connection 28,11), or NRA is maximised (connections 18,19 and 26,18), or NRL is minimised (connection 26,11).

TABLE 2 Single-objective results based on per unit calculations

TABLE 2 (Continued)

Potential Tie Switch Location (Target Nodes)	NRC	NRS	NRA	NRL	Optimal for
11,19	15.309	4.667	0.621	5.674	
11,20	15.309	4.667	0.621	5.674	
11,21	15.309	4.667	0.621	5.674	
11,22	15.309	4.667	0.621	5.674	
12,19	16.265	5.969	0.977	6.066	
12,20	16.265	5.969	0.977	6.066	
12,21	16.265	5.969	0.977	6.066	
12,22	16.265	5.969	0.977	6.066	
13,19	16.712	6.686	0.784	6.188	
13,20	16.712	6.686	0.784	6.188	
13,21	16.712	6.686	0.784	6.188	
13,22	16.712	6.686	0.784	6.188	
14,19	17.238	7.431	0.630	6.059	
14,20	17.238	7.431	0.630	6.059	
14,21	17.238	7.431	0.630	6.059	
14,22	17.238	7.431	0.630	6.059	
15,19	18.457	8.632	1.118	6.577	
15,20	18.457	8.632	1.118	6.577	
15,21	18.457	8.632	1.118	6.577	
15,22	18.457	8.632	1.118	6.577	
16,19	19.255	9.576	1.162	6.403	
16,20	19.255	9.576	1.162	6.403	
16,21	19.255	9.576	1.162	6.403	
16,22	19.255	9.576	1.162	6.403	
17,19	20.007	10.293	1.158	6.213	
17,20	20.007	10.293	1.158	6.213	
17,21	20.007	10.293	1.158	6.213	
17,22	20.007	10.293	1.158	6.213	
18,19	21.383	11.502	1.889	6.483	NRC, NRA
18,20	21.383	11.502	1.889	6.483	NRC
18,21	21.383	11.502	1.889	6.483	NRC
18,22	21.383	11.502	1.889	6.483	NRC
26,11	15.725	4.872	1.037	3.747	NRL
26,12	16.377	5.844	1.089	4.021	
26,13	17.165	6.933	1.237	4.719	
26,14	17.932	8.037	1.324	4.994	
26,15	18.197	8.598	0.858	4.910	
26,16	18.842	9.027	0.749	5.048	
26,17	20.196	10.265	1.347	5.749	

Potential Tie Switch Location (Target Nodes)	NRC	NRS	NRA	NRL	Optimal for
26,18	20.971	11.133	1.477	5.594	NRC, NRA
27,11	15.229	4.471	0.506	3.367	
27,12	15.719	5.225	0.387	3.460	
27,13	17.182	6.914	1.199	4.812	
27,14	17.528	7.463	0.848	4.724	
27,15	18.177	8.383	0.741	5.012	
27,16	19.127	9.459	0.891	5.293	
27,17	19.806	9.846	0.725	5.365	
27,18	21.346	11.345	1.397	6.030	NRC
28,11	15.755	4.826	1.002	4.403	NRS
28,12	15.780	5.847	0.413	3.901	
28,13	16.618	6.387	0.592	4.564	
28,14	17.116	7.146	0.382	4.512	
28,15	18.413	9.163	0.908	5.214	
28,16	18.971	8.962	0.640	5.309	
28,17	20.628	10.548	1.407	6.254	
28,18	21.369	11.561	1.193	6.038	NRC
29,11	15.960	5.595	1.183	5.011	
29,12	16.261	5.907	0.865	4.743	
29,13	16.472	6.453	0.412	4.651	
29,14	18.002	8.179	1.226	5.572	
29,15	18.765	9.024	1.208	5.785	
29,16	19.528	9.847	1.129	5.827	
29,17	20.188	10.271	0.874	5.801	
29,18	20.917	11.208	0.604	5.510	NRC
30,11	15.210	4.850	0.413	4.522	
30,12	16.162	6.346	0.743	4.896	
30,13	16.650	6.865	0.562	4.995	

Potential Tie switch Location (Target nodes)	NRC	NRS	NRA	NRL	Optimal for
30,14	17.899	8.360	1.089	5.568	
30,15	18.789	9.502	1.191	5.778	
30,16	19.047	9.252	0.597	5.428	
30,17	20.208	10.656	0.828	5.736	
30,18	21.272	11.504	0.868	5.906	NRC
31,11	15.198	5.100	0.383	5.112	
31,12	16.679	6.268	1.239	5.781	
31,13	17.306	7.325	1.195	5.980	
31,14	17.204	7.430	0.366	5.135	

T A B L E 2   (Continued)

Potential Tie switch Location (Target nodes)	NRC	NRS	NRA	NRL	Optimal for
31,15	18.636	9.120	1.006	5.775	
31,16	19.370	9.988	0.881	5.707	
31,17	20.567	10.371	1.137	6.332	
31,18	21.719	11.618	1.250	6.404	NRC
32,11	16.029	5.806	1.199	6.060	
32,12	16.237	5.941	0.780	5.490	
32,13	17.108	7.576	0.977	5.939	
32,14	17.724	8.215	0.864	5.729	
32,15	18.590	9.219	0.934	5.747	
32,16	19.038	9.602	0.517	5.420	
32,17	20.517	10.917	1.048	6.088	
32,18	21.344	11.071	0.826	6.195	NRC
33,11	15.577	5.286	0.734	5.783	
33,12	16.124	6.119	0.652	5.562	
33,13	16.880	7.409	0.732	5.831	
33,14	17.763	7.939	0.883	5.858	
33,15	18.208	8.351	0.530	5.486	
33,16	18.895	9.569	0.348	5.278	
33,17	19.936	10.237	0.436	5.555	
33,18	21.314	11.301	0.758	6.070	NRC

Abbreviations: NRC, nodal restoration criticality; NRC, nodal robustness; NRA, nodal restorability; NRL, nodal restoration losses.
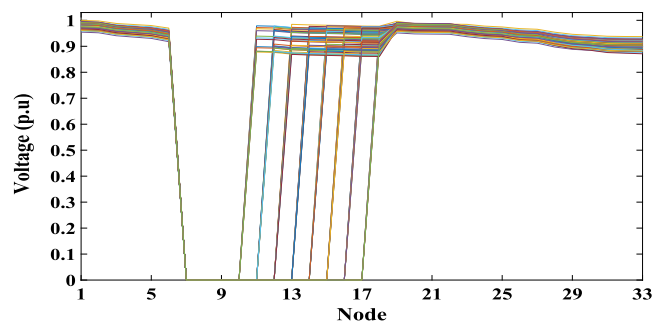

F I G U R E 6   Voltage profile in the IEEE 33-bus system for 96 Tie switch locations during the restoration process

The statistical comparison of the proposed indices is tabulated in Table 3. *NRC* varies between 15.2 and 21.72 with multiple candidates capable of providing a solution for improving criticality covered in the restoration plan. NRS ranges between 4.47 and 11.62 with mean value of 8.20, which includes candidates with strong resourcefulness. *NRA* changes between 0.35 and 1.89 with multiple solutions with a reasonable restorability. *NRL* ranges between 3.37 and 6.58 with candidates for minimum losses in the restoration.

T A B L E 3   Statistical comparison of resilience metrics for 33-bus test system

Performance index	*NRC*	*NRS*	*NRA*	*NRL*
Minimum	15.20	4.47	0.35	3.37
Maximum	21.72	11.62	1.89	6.58
Mean	18.15	8.20	0.93	5.62
Standard deviation	1.90	2.11	0.34	0.72

Abbreviations: NRC, nodal restoration criticality; NRC, nodal robustness; NRA, nodal restorability; NRL, nodal restoration losses.

The single-objective optimisation in this paper has achieved a wide range of restorative loss reduction, or restorative capacity enhancement. For instance, the reduction achieved in Reference [39] for a 52-bus system is 5.8%, while the range of restoration losses in single-objective solutions for NRL in this paper varies in a higher range (changing from 3.06 p.u to 6.57 p.u—53.4% reduction between the worst and the best Tie location candidate). The same applies to the range of restorability achieved in this paper, with a high range between 0.2 p.u to 1.36 p.u (85.2% enhancement between the worst and the best Tie location candidates), while in Reference [40], the restorative capacity enhancement for the IEEE 118-bus test system is limited to 4.26%. Critical load restoration has been considered as a single-objective optimisation problem in Reference [41] on a 1069-bus test system. Improvement of critical load restoration in Reference [41] heavily relies on the number of Microgrids connected to the restoration paths. Therefore, the outcome of the optimisation problem is limited to eight restoration paths including four critical loads, while the proposed single-objective optimisation in this paper for NRC can cover widespread range of critical loads distributed in a larger area of the network. This is achieved by considering 96 restoration paths for IEEE 33-bus system to find the optimal location of Tie switches for maximised coverage of the node criticality.

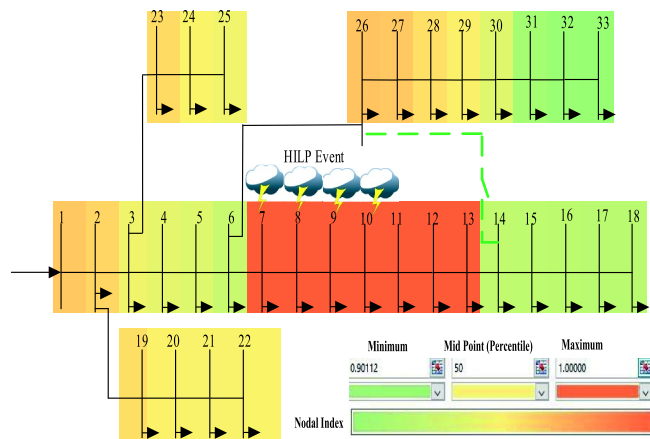## 4.2 | Fuzzy satisfying method-based multi-objective decision making

The proposed objective functions are jointly taken into account in order to achieve a final optimal solution. As there is no unique solution for a multi-objective problem, the FSM fulfils an objective judgement within a set of optimal Pareto solutions to achieve a trade-off and differentiate the Tie switch placement candidates in the optimal Pareto front [34,42]. The satisfaction levels (desired reference values) for each objective function should be determined by the decision maker (e.g. electric utility). The final results on the optimal allocation of the Tie switches are achieved following the FSM process with various satisfaction levels (see Table 4). From the numerical results presented in Table 4, it could be inferred that the final optimal solution relies heavily on the user-defined satisfaction levels (μ_{d1} to μ_{d4}) selected for each objective function.There are two objective functions to be minimised—system-wide

performance degradation NRS (f_1 associated with μ_{d1}) and restoration losses NRL (f_2 associated with μ_{d2})—and two objective functions to be maximised—system-wide restorability NRA (f_3 associated with μ_{d3}) and restoration criticality NRC (f_4 associated with μ_{d4}). As a consequence, higher satisfaction levels for f_1 and f_2 (μ_{d1} and μ_{d2}) results in these two objective functions to be more dominant and higher satisfaction levels for f_3 and f_4 (μ_{d3} and μ_{d4}) are desirable in the final decision. To provide the reader with a better understanding of the proposed decision making platform, the following example is presented: if the user decides on $\mu_{d3} = 1$ and μ_{d1}, μ_{d2}, $\mu_{d4} = 0$, the system wide restorability (NRA) is the only objective function reflected in the final decision. In this particular case, μ_{d3} is set to the highest value which is not desired for this objective function (NRA) and the decision would be to connect Nodes 26–18 with a Tie switch placement, which restores the lowest amount of loads. The user can tune the satisfaction levels and objective functions to meet the desired decision requirements.

Figure 7 demonstrates the NRS in the network under test for the optimal solution with satisfaction levels of $\mu_{d1} = 0.8$, $\mu_{d2} = 0.8$, $\mu_{d3} = 1$, $\mu_{d4} = 0.6$. As reported in Table 4, such satisfaction levels result in a connection between Nodes 26–14 as the most optimal location for the Tie switch. The colours in Figure 7 depict the NRS, where a lower nodal performance deviation reflects a higher robustness (dark green). The HILP-heavily-affected nodes have the highest performance deviations and are dressed by colours in red.

4.3 | Applicability on larger networks

In order to verify the applicability of the proposed framework on larger networks, this subsection provides the results when the proposed approach is implemented on the IEEE-69 bus test system. The network under test is depicted in Figure 8 with an HILP scenario affecting Nodes 14-to-21.

The proposed framework from PPF to index calculation is conducted on the IEEE 69-bus system and the results are demonstrated in Figure 9. Figure 9(a)–9(d) illustrate the criticality covered by the restoration plans, system-wide robustness, restorability, and restoration losses, for each Tie switch placement candidate, respectively. The statistical comparison of these indices is tabulated in Table 5. It could be observed from Figure 9(a) that the NRC varies from 12.04 to 15.84 with some candidates providing acceptable demand criticality covered by the restoration process. Figure 9(b) and 9(c) illustrate the system robustness and restorability with multiple candidates capable of providing a reasonable solution for maximum amount of loads to be restored and minimum difference with the pre-event system profile. Figure 9(d) introduces the candidates with relatively low

TABLE 4 Final resilience-oriented allocation of tie switches in 33-bus test system

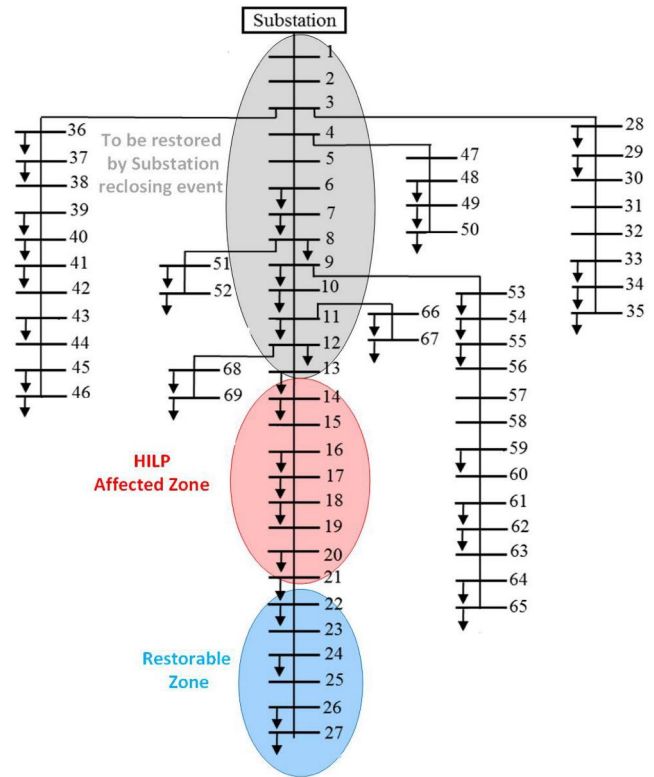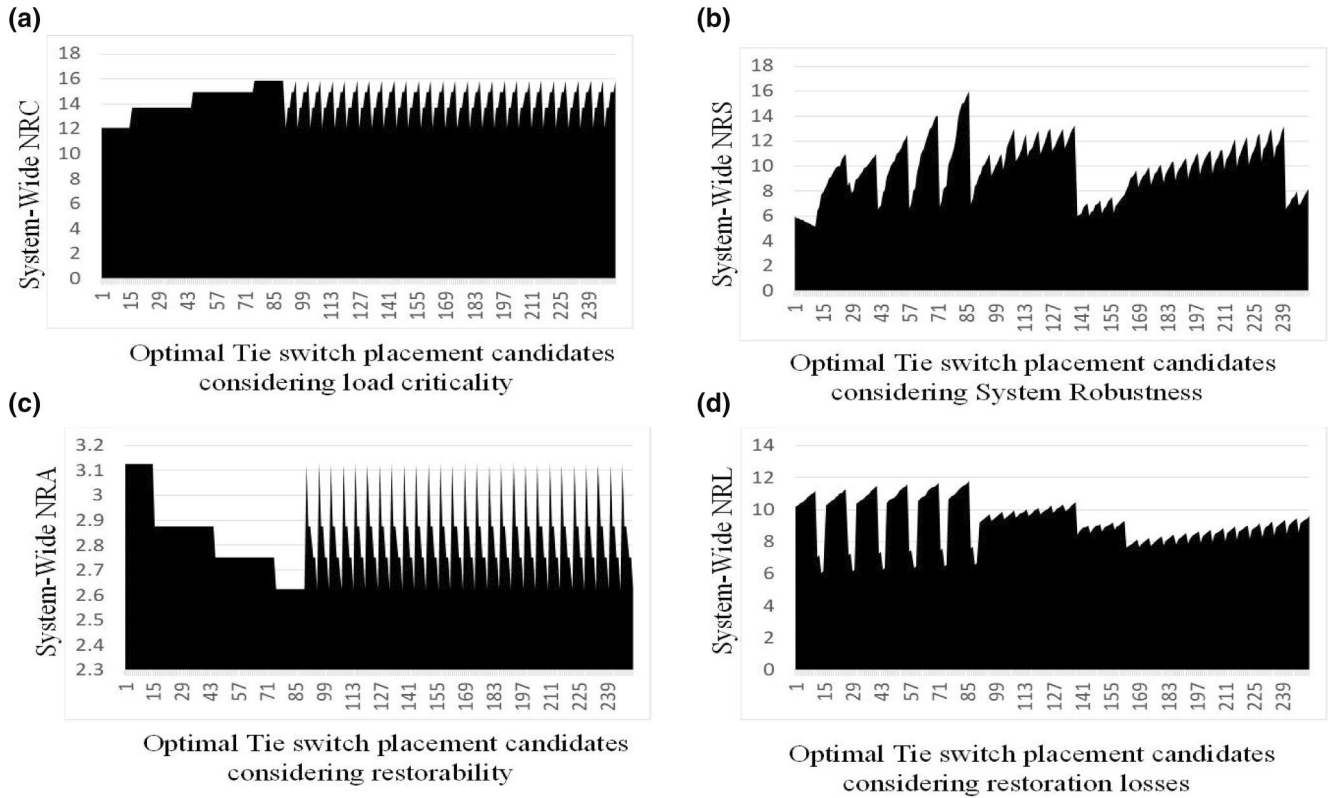| Satisfaction Levels				Objective function value				Final Tie switch location
μ_{d1}	μ_{d2}	μ_{d3}	μ_{d4}	f_1	f_2	f_3	f_4	
0.8	0.8	1	0.6	8.037	4.994	1.324	17.932	26-14
0.8	0.8	0.8	0.8	9.027	5.048	0.749	18.842	26-16
1	1	0.6	0.6	6.933	4.719	1.231	17.165	26-13
0.6	0.6	0.6	0.4	8.598	4.910	0.858	18.197	26-15

FIGURE 7 Nodal robustness for the optimal planning scenario with a Tie switch placed between Nodes 26–14

FIGURE 8 Case study with larger number of nodes—IEEE 69-bus test system

FIGURE 9 System-wide performance evaluation of the IEEE 69-bus test system for Tie switch placement candidates considering: (a) load criticality, (b) robustness, (c) restorability, and (d) restoration losses

TABLE 5 Statistical comparison of resilience metrics in IEEE 69-bus test system

Performance Index	NRC	NRS	NRA	NRL
Minimum	12.04	5.18	2.62	6.05
Maximum	15.84	15.99	3.12	11.77
Mean	14.19	9.81	2.83	9.27
Standard deviation	1.51	2.31	0.23	1.43

Abbreviations: NRC, nodal restoration criticality; NRC, nodal robustness; NRA, nodal restorability; NRL, nodal restoration losses.

TABLE 6 Final resilience-oriented allocation of the Tie switch for 69-bus system

Satisfaction levels				Objective function value				Final Tie switch location
μ_{d1}	μ_{d2}	μ_{d3}	μ_{d4}	f_1	f_2	f_3	f4	
0.8	0.8	1	0.6	13.689	6.612	3.125	8.851	49-22
0.8	0.8	0.8	0.8	12.045	6.894	2.875	7.371	52-23
1	1	0.6	0.6	13.689	6.112	2.750	8.651	46-24
0.6	0.6	0.6	0.4	14.954	9.998	2.875	9.512	50-26

restoration losses with system-wide NRL ranging between 6.05 and 11.77 per unit. The same FSM multi-objective optimisation approach is implemented in the IEEE 69-bus test system as well. Satisfaction levels are user defined and could be tuned depending on the priorities of the electric utilities for the proposed indices. However, for the sake of consistency in the paper and in order to be able to compare the results with those of the IEEE 33-bus test system, the same satisfaction levels (μ_1-to-μ_4) are selected.

The final results of the multi-objective optimisation and the satisfaction levels are summarised in Table 6. Satisfaction levels in the first row of the table give more importance to restorability ($\mu_3 = 1$) and less importance to restoration losses ($\mu_3 = 0.6$) with moderate satisfaction levels for criticality and

robustness. Therefore, the optimal connection by the framework resulted in 49-22 to cover maximum loads. Satisfaction levels in the second row of Table 6 are distributed equally at a moderate level ($\mu_1 = \mu_2 = \mu_3 = \mu_4 = 0.8$). This has resulted in Tie switch connection between Nodes 52-23, where there is a trade off between all restoration losses, number of restored loads, criticality, and robustness. The third row in Table 6 represents the scenario of allocating less priority to restoration losses and restorability while robustness and criticality covered in restoration plan are given full attention. This scenario has led to a connection between 46-24. Finally, in the last row of the table, lower satisfaction levels are applied to all proposed indices with lowest attention (among all satisfaction levels) allocated to the restoration losses

$(\mu_4 = 0.4)$. This condition has resulted in Tie connection of Nodes 50-26.

5 | DISCUSSION

It must be noted that this work has focussed on the planning phase where the planning authorities have a limited budget for installation of Tie switches in the distribution network. The indices calculated for every possible location of Tie switches in the network could be ranked (ascending for NRC and NRA and descending for NRS and NRL). Depending on the available resources and the number of the Tie switches, which are decided to be installed by the electric utility, the highest ranked indices could be selected as the input to the FSM algorithm. The proposed analytics are generic enough to accommodate any budget considerations and any number of Tie switches to be installed for structural hardening and resilience. Here are the presumptions for the developed decision making platform:

- The proposed framework in this paper focuses on radially operated power distribution networks. Therefore, the restoration plans considered here are fully achieved by network reconfiguration through operation of Tie switches between the adjacent feeders, while preserving the default generator dispatch schedules. Hence, generator synchronisation challenges during the restoration process (especially during cold load pickup) are out of the scope of this framework. The main goal is to optimise the location of the Tie switches as a part of the network hardening planning schemes.
- The metrics, objective functions, and constraints in the proposed model are developed with regards to the balanced distribution networks. However, the framework is generic enough and can be applied to unbalanced distribution systems with the following adjustments: (a) Active power losses in unbalanced distribution networks will be increased due to higher active losses of the distribution transformers. Therefore, a safety margin needs to be added to the resilience metric related to the restoration losses. (b) All constraints relevant to nodal voltage robustness, which compare the voltage profiles before and following a major HILP disturbance, need to consider three-phase voltage unbalance conditions caused by unbalanced loads. In other words, power balance equations in this work have to be modified to encompass single-phase load balance models as well. (c) All power flow equations must be modified to contain the current flow in neutral points of the distribution networks. In addition, a new constraint is required to limit the current flow in the neutral points to avoid neutral over-current conditions. An example linear power flow model for three-phase unbalanced systems is proposed in Reference [43]. (d) When considering the contributions from Distributed Energy Resources (DERs) under unbalanced operation, conditions are subjected to various constraints (e.g. current unbalance constraint, ramping rate constraint, and output limit constraint) [43]. Therefore, additional challenges may exist for problem formulation under a multi-objective optimisation setting.

TABLE 7 Computational performance of the proposed framework in seconds

	IEEE 33 Bus system	IEEE 69 Bus system
Single-objective	00:41.34	01:11.85
Multi-objective	00:59.11	01:48.97

The computational efficiency of the framework has not been a major concern in this work, as it focuses on planning phase; however, it is assessed by the time that CPU needs to run the algorithm. The average CPU run time at each core for completion of the algorithm in MATLAB is reported in Table 7 for different scenarios.

6 | CONCLUSION

In this paper, a multi-objective decision making framework for resilience-oriented optimisation and planning in power distribution grids is proposed. This framework employs a k-PEM-based PPF and a FSM to find out the desirable reconfiguration plan by optimally allocating the Tie switches across the network for maximised preparedness against HILP events. In order to characterise the optimal restoration plan, several resilience features are introduced and quantified at both nodal and system levels. This includes proposed metrics on system robustness, load criticality covered by a restoration plan, restoration losses, and recovered capacity. A dynamic admittance matrix is used as the input to the k-PEM based PPF, which allows the Tie switches to move between all possible pairs of nodes to build a complete set of restoration scenarios. The generated set of HILP restoration scenarios will then be assessed by calculation of the proposed resilience metrics to find out the optimal location of the Tie switches.

Effectiveness of the proposed framework, which aims to provide the distribution utilities with visions for network hardening planning against HILP events, is tested on the IEEE 33-bus test system, and a detailed discussion on the numerical results was provided. In order to verify applicability of the proposed framework on larger networks, the framework is tested on the IEEE 69-bus test system, and the results were thoroughly discussed. Numerical results prove the effectiveness of the proposed platform on both small scale and large scale systems with benefits for end users and utilities.

Future research and development efforts could be directed towards application of the developed decision making platform in highly meshed and unbalanced power distribution

networks. This requires modifications in the proposed resilience metrics and power flow equations considered in this work.

ORCID

Payman Dehghanian ![ORCID] https://orcid.org/0000-0003-2237-4284

REFERENCES

1. Panteli, M., Mancarella, P.: The grid: stronger, bigger, smarter?: presenting a conceptual framework of power system resilience. IEEE Power Energy Mag. 13(3), 58–66 (2015)
2. Dehghanian, P., Aslan, S., Dehghanian, P.: Maintaining electric system safety through an enhanced network resilience. IEEE Trans. Ind. Appl. 54(5), 4927–4937 (2018)
3. Nazemi, M., Moeini-Aghtaie, M., Fotuhi-Firuzabad, M., Dehghanian, P.: Energy storage planning for enhanced resilience of power distribution networks against earthquakes. IEEE Trans. Sust. Energy. 11(2), 795–806 (April 2020)
4. Wang D., et al.: Power grid resilience to electromagnetic (EMP) disturbances: a literature review. In: The 51st North American power Symposium (NAPS), pp. 1–6. (2019)
5. Wang, S., et al.: A machine learning approach to detection of geomagnetically-induced currents in power grids. IEEE Trans Ind. Appl. 56(2), 1098–1106 (March/April 2020)
6. Jamborsalamati, P., et al.: A framework for evaluation of power grid resilience case study: 2016 south australian blackout. In 2018 IEEE International Conference on Environment and Electrical Engineering and 2018 IEEE Industrial and Commercial Power Systems Europe (EEEIC/ I&CPS Europe), pp. 1–6. IEEE (2018)
7. Haes Alhelou, H., et al.: A survey on power system blackout and cascading events: research motivations and challenges. Energies. 12(4), 682 (2019)
8. Dehghanian, P.: Power system topology control for enhanced resilience of smart electricity grids. Ph.D. dissertation, Texas A&M University (2017)
9. Bajpai, P., Chanda, S., Srivastava, A.K.: A novel metric to quantify and enable resilient distribution system using graph theory and choquet integral. IEEE Trans. Smart Grid. 9(4), 2918–2929 (2018)
10. Farzin, H., Fotuhi-Firuzabad, M., Moeini-Aghtaie, M.: Enhancing power system resilience through hierarchical outage management in multi-microgrids. IEEE Trans. Smart Grid. 7(6), 2869–2879 (2016)
11. Gao, H., et al.: Resilience-oriented critical load restoration using microgrids in distribution systems. IEEE Trans. Smart Grid. 7(6), 2837–2848 (2016)
12. Mousavizadeh, S., Haghifam, M.-R., Shariatkhah, M.-H.: A linear two-stage method for resiliency analysis in distribution systems considering renewable energy and demand response resources. Appl. Energ. 211, 443–460 (2018)
13. Khodaei, A.: Resiliency-oriented microgrid optimal scheduling. IEEE Transactions on Smart Grid. 5(4), 1584–1591 (2014)
14. Wei, Y., et al.: Dynamic modelling and resilience for power distribution. In: IEEE International Conference on Smart Grid Communications (SmartGridComm), pp. 85–90 (2013)
15. Ji, C., Wei, Y.: Dynamic resilience for power distribution and customers. In: 2015 IEEE International Conference on Smart Grid Communications (SmartGridComm), pp. 822–827. IEEE (2015)
16. Watson, J.-P., et al.: Conceptual framework for developing resilience metrics for the electricity, oil, and gas sectors in the United States. Tech. Rep.,Sandia National Laboratories, Albuquerque, NM (United States) (2014)
17. Zhang, H., et al.: Quantitative resilience assessment under a tri-stage framework for power systems. Energies. 11(6), 1427 (2018)
18. Kwasinski, A.: Quantitative model and metrics of electrical grids' resilience evaluated at a power distribution level. Energies. 9(2), 93 (2016)
19. Gao, H., Chen, Y., Mei, S., Huang, S., Xu, Y.: Resilience-oriented pre-hurricane resource allocation in distribution systems considering electric buses. Proc IEEE. 105(7), 1214–1233 (2017)
20. Jamborsalamati, P., Hossain, M., Taghizadeh, S., Sadu, A., Konstantinou, G., Manbachi, M., et al: Enhancing power grid resilience through an IEC61850-based ev-assisted load restoration. IEEE Trans. Ind. Inform. 16(3), 1799–1810 (March 2020)
21. Chen, C., Wang, J., Ton, D.: Modernising distribution system restoration to achieve grid resiliency against extreme weather events: an integrated solution. Proc IEEE. 105(7), 1267–1288 (2017)
22. Zhang, B., Dehghanian, P., Kezunovic, M.: Optimal allocation of pv generation and battery storage for enhanced resilience, 10, 535–545. IEEE Trans. Smart Grid (2017)
23. Dehghanian, P., Zhang, B., Dokic, T., Kezunovic, M.: Predictive risk analytics for weather-resilient operation of electric power systems. IEEE Trans. Sust. Energ. 10(1), 3–15 (2019)
24. Jooshaki, M., Karimi-Arpanahi, S., Lehtonen, M., Millar, R.J., Fotuhi-Firuzabad, M.: Reliability-oriented electricity distribution system switch and tie line optimization. IEEE Access. 8, 130967–130 978 (2020)
25. Aman, M.M., et al.: Optimum tie switches allocation and DG placement based on maximisation of system loadability using discrete artificial bee colony algorithm. IET Gener., Trans. Distrib. 10(10), 2277–2284 (2016)
26. Nascimento Alves, H.: A hybrid algorithm for optimal placement of switches devices in electric distribution systems. IEEE Lat. Am. Trans. 10(6), 2218–2223 (2012)
27. Ghoreishi, H., Afrakhte, H., Jabbari Ghadi, M.: "Optimal placement of tie points and sectionalizers in radial distribution network in presence of dgs considering load significance," In: 2013 Smart grid Conference (SGC), pp. 160–165. (2013)
28. Aien, M., Fotuhi-Firuzabad, M., Aminifar, F.: Probabilistic load flow in correlated uncertain environment using unscented transformation. IEEE Trans. Power Syst. 27(4), 2233–2241 (2012)
29. Dehghanian, P., et al.: Optimal siting of dg units in power systems from a probabilistic multi-objective optimization perspective. Int. J. Electr. Power Energy Syst. 51, 14–26 (2013)
30. Sanabria, L., Dillon, T.: Stochastic power flow using cumulants and von mises functions. Int. J. Electr. Power Energy Syst. 8(1), 47–60 (1986)
31. Terzioğlu, R., Çavuş, T.F.: Probabilistic load flow analysis of the 9 bus WSCC system. Int. J. Sci. Res. Pub. 3(9), 1–4 (2013)
32. Verbic, G., Canizares, C.A.: Probabilistic optimal power flow in electricity markets based on a two-point estimate method. IEEE Trans. Power Syst. 21(4), 1883–1893 (2006)
33. Maghouli, P., et al.: A multi-objective framework for transmission expansion planning in deregulated environments. IEEE Trans. Power Syst. 24(2), 1051–1061 (2009)
34. Srinivas, N., Deb, K.: Muiltiobjective optimization using nondominated sorting in genetic algorithms. Evol. Comput. 2(3), 221–248 (1994)
35. Bath, S., Dhillon, J., Kothari, D.: Fuzzy satisfying stochastic multi-objective generation scheduling by weightage pattern search methods. Elec. Power Syst. Res. 69(2–3), 311–320 (2004)
36. Chen, Y.-L., Liu, C.-C.: Interactive fuzzy satisfying method for optimal multi-objective var planning in power systems. IET Gener. Transm. Distrib. 141(6), 554–560 (1994)
37. Nojavan, S., Majidi, M., Najafi-Ghalelou, A., Ghahramani, M., Zare, K.: A cost-emission model for fuel cell/pv/battery hybrid energy system in the presence of demand response programme: ε-constraint method and fuzzy satisfying approach. Energy Convers Manag. 138, 383–392 (2017)
38. Wazir, A., Arbab, N.: Analysis and optimization of IEEE 33 bus radial distributed system using optimization algorithm. J. Emerg. Trends Appl. Eng. 1(2), 17–21 (2016)
39. Melo, P., Matos, M.: Multi-objective reconfiguration for loss reduction and service restoration using simulated annealing. In: International Conference on Electric Power Engineering, PowerTech Budapest. Hungary. (1999)
40. Dehghanian, P., Aslan, S., Dehghanian, P.: "Quantifying power system resiliency improvement using network reconfiguration. In: 2017 IEEE 60th International Midwest Symposium on Circuits and Systems (MWSCAS), pp. 1364–1367. IEEE (2017)

41. Xu, Y., et al.: Microgrids for service restoration to critical load in a resilient distribution system. IEEE Trans. Smart Grid. 9(1), 426–437 (2016)

42. Marler, R.T., Arora, J.S.: Survey of multi-objective optimization methods for engineering. Struct. Multidiscip. Optim. 26(6), 369–395 (2004)

43. Chen, B., et al.: Sequential service restoration for unbalanced distribution systems and microgrids. IEEE Trans. Power Syst. 33(2), 1507–1520 (2017)